

Expanded View Figures

Figure EV1. Co-localization of the proteins in the pseudouridylation module with mitochondrial RNA granules.

Flp-In T-REx 293 cells transduced with a ProteinX-BirA*-FLAG construct were treated with tetracycline for 24 h to induce expression of the protein, and the co-localization of ProteinX (anti-FLAG antibody) with a mtRNA granule protein (anti-GRSF1) was visualized by immunofluorescence. All proteins in the pseudouridylation module co-localized with GRSF1, albeit to various extents. Scale bars: 10 μ m.



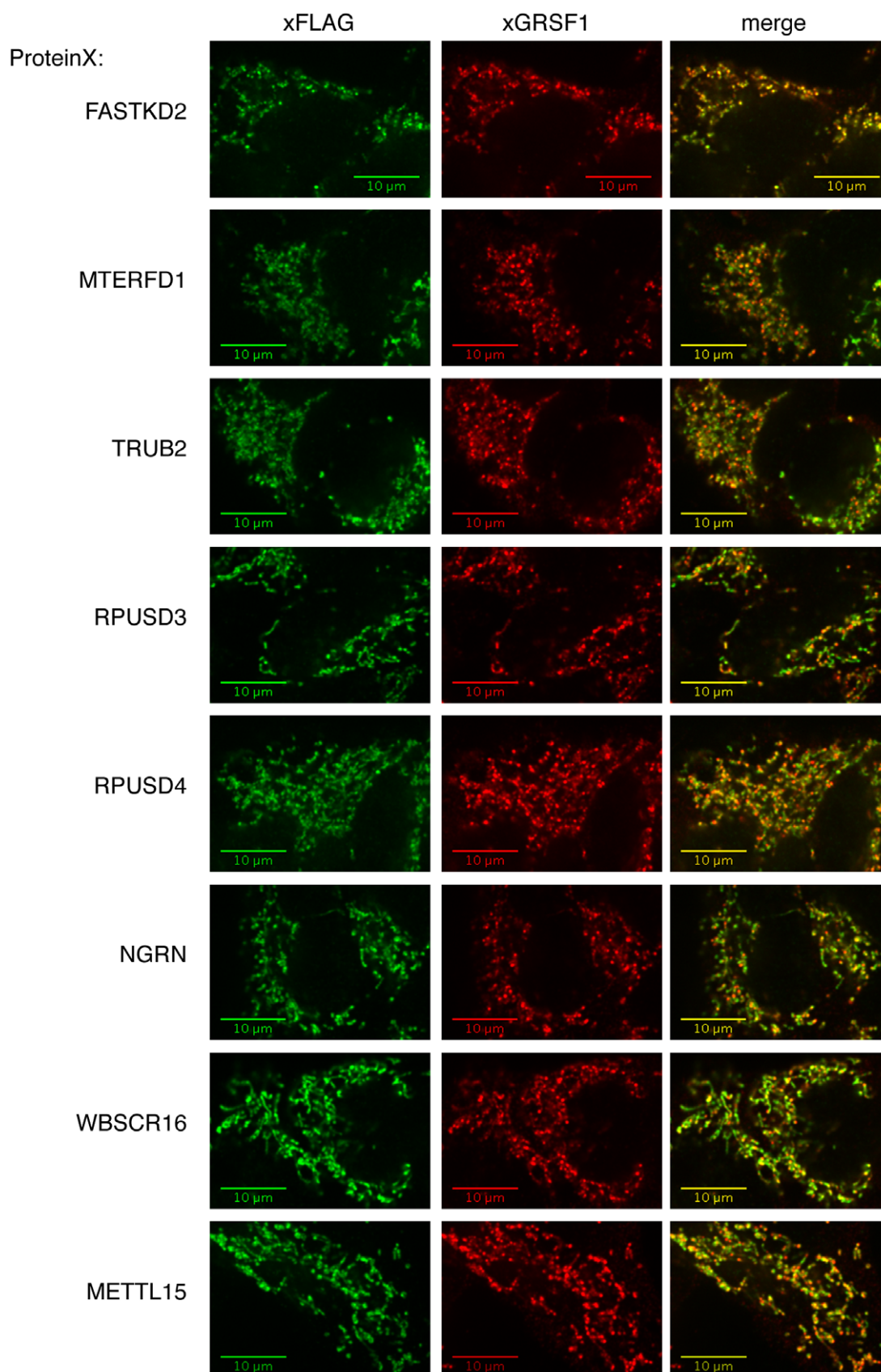


Figure EV1.

Figure EV2. Quantification of the levels of pseudouridine synthase interacting proteins, the rate of mitochondrial translation, and the levels of 12S and 16S rRNA in siRNA-treated cells.

- A Quantification of the levels of individual pseudouridine synthase interacting proteins normalized to SDHA in cells treated with siRNA. The graph represents the relative protein levels compared to controls. The bars represent mean \pm SEM of 4–13 independent experiments.
- B Quantification of the synthesis of individual mitochondria-encoded polypeptides in siRNA-treated cells. The graph represents the relative levels compared to controls. The bars represent mean \pm SEM of 2–4 independent experiments.
- C qRT–PCR analysis of 12S and 16S rRNA in siRNA-treated cells. The graph represents the relative levels compared to controls. The bars represent mean \pm SEM of 2–3 independent experiments.

Data information: *P*-values were calculated using a paired two-tailed *t*-test (**P* < 0.05; ***P* < 0.01; ****P* < 0.001).

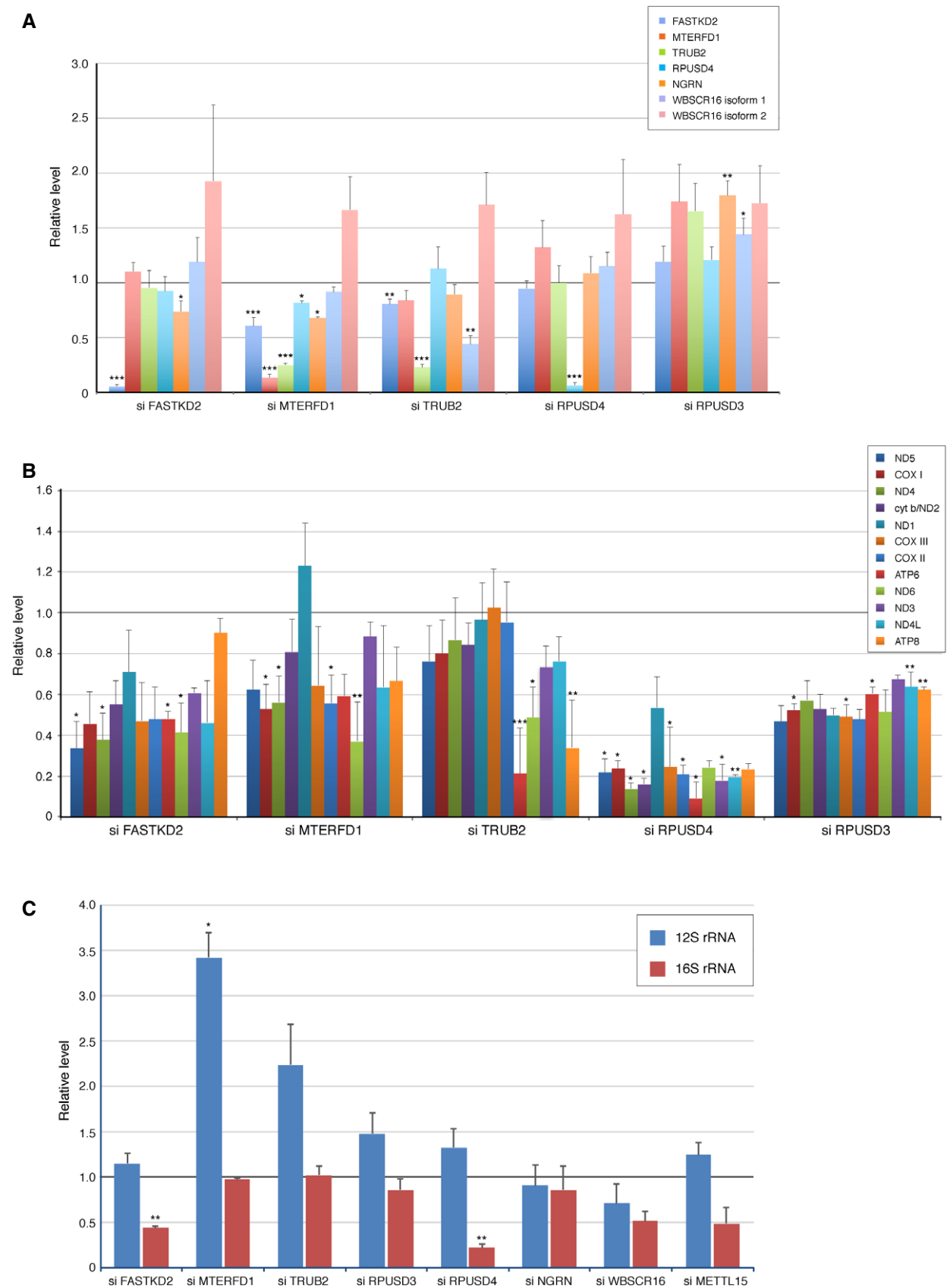


Figure EV2.

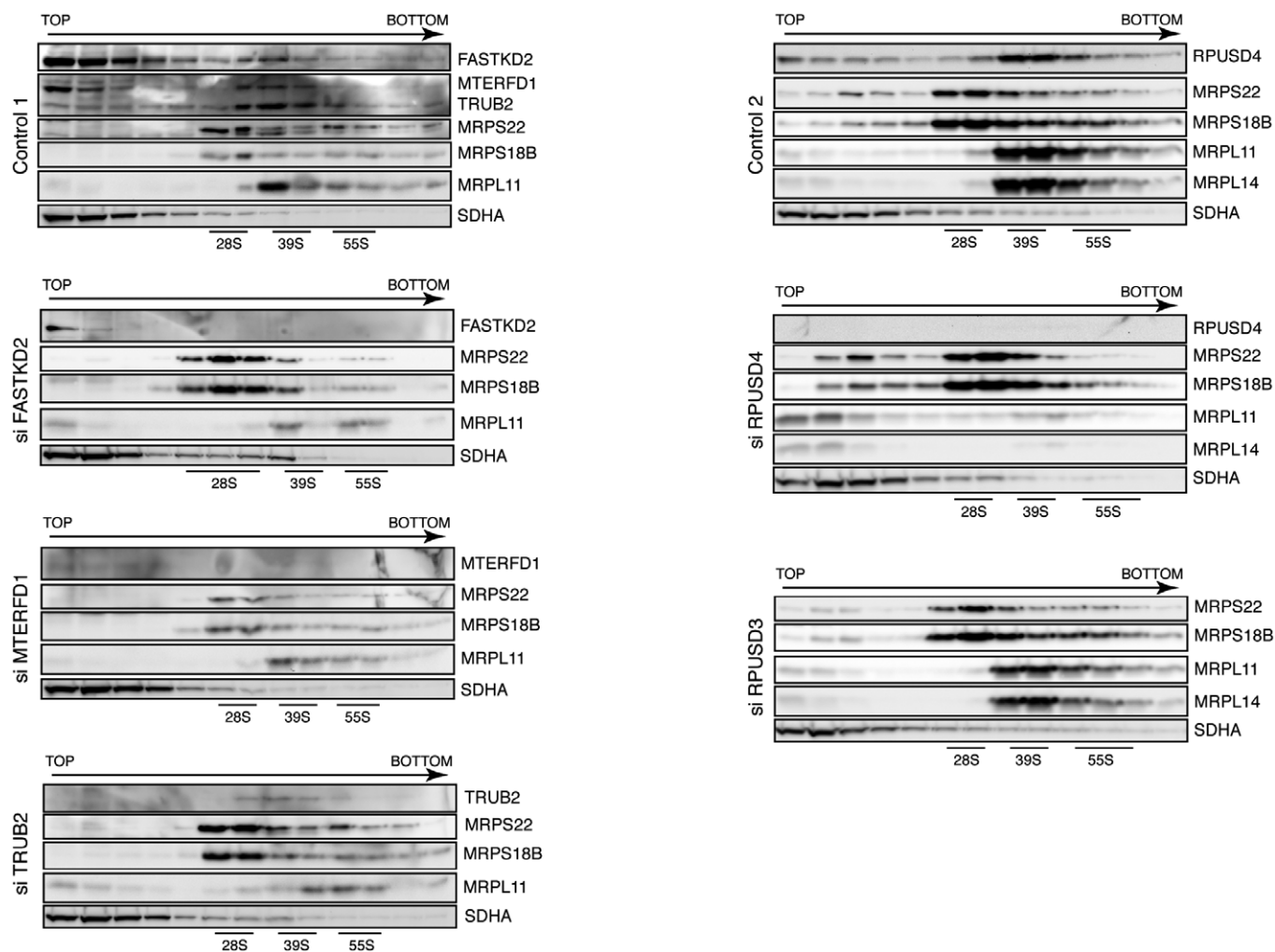
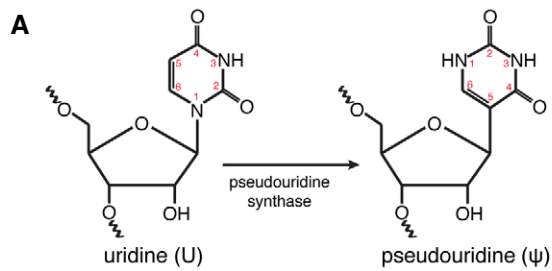
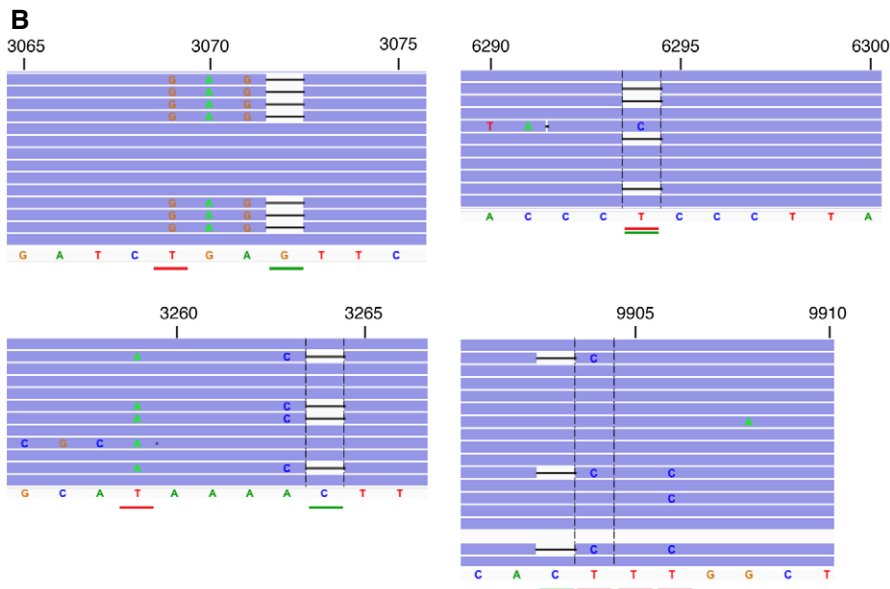


Figure EV3. Assembly of the mitochondrial ribosome.

Depletion of the pseudouridine synthases TRUB2 and RPUSD4 leads to an impaired assembly of the mitochondrial ribosome. Individual fractions from a sucrose gradient centrifugation of mitochondria isolated from control and siRNA-treated cells were separated by 12.5% SDS-PAGE and immunoblotted for the indicated mitochondrial ribosomal proteins and pseudouridine synthase interacting proteins. SDHA was used as a loading control. The migrations of the mt-SSU (28S), the mt-LSU (39S), and the mitochondrial monosome (55S) are indicated. Some of the panels in control 1 and control 2 are identical to those shown in Fig 3A in the main text.

**Figure EV4. Pseudouridine modification.**

- A A schematic of an enzymatic reaction of pseudouridine (ψ) synthesis by pseudouridine synthase.
- B IGV screenshot of reads in CMC-treated samples mapping to the top four pseudouridylated sites. The position of the deletion is underlined in green, and the putative pseudouridylated site is underlined in red.

**Figure EV5. Primary and secondary structures of the pseudouridine sequence motif.**

- A Sequence motifs surrounding the mitochondrial ψ sites generated by WebLogo software at <http://weblogo.berkeley.edu>. Three motifs are suggested for the top four ψ sites, because the COXIII (ψ 9904–9906) position is uncertain due to the ambiguity of the sequence alignments.
- B–D Positions of identified ψ sites (red rectangle) within the secondary structures of individual RNAs. (B) Known secondary structure of the 3'-terminus of 16S rRNA [37] and predicted structures for COXI (C) and COXIII mRNAs (D). Predictions were based either on sequence fragments of 100 nt and 200 nt surrounding each ψ site, or using the whole mRNA molecule as the input. Pseudouridine is predicted to be accessible in all cases, located at a loop or in the boundary between a stem and a loop/bulge structure.

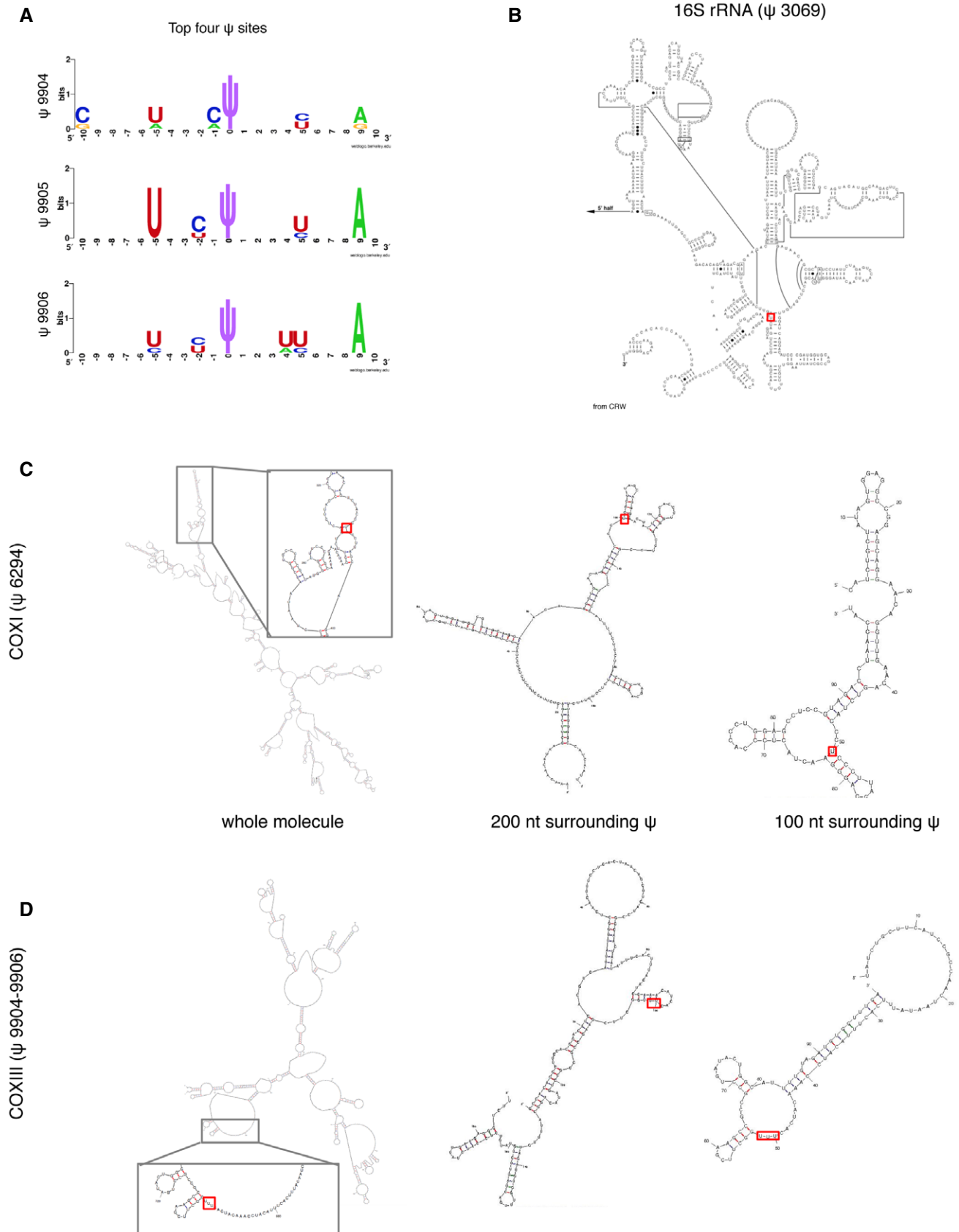


Figure EV5.